Highly Active and Selective Nickel–Cerium(IV) Oxide Catalyst for Water–Gas Shift Reaction

Luhui Wang and Yuan Liu*
Department of Catalysis Sciences and Technology, School of Chemical Engineering, Tianjin University, Tianjin 300072, P. R. China

(Received October 15, 2007; CL-071128; E-mail: yuanliu@tju.edu.cn)

$Ni–CeO_2$ catalyst prepared by coprecipitation–nitric-acid-leaching method was highly active and selective for high-temperature water–gas shift reaction in reforming. TPR and XRD results suggested that the high activity for water–gas shift reaction was attributed to high amounts of Ni^{2+} ions incorporated into CeO_2 lattice in the catalyst.

Water–gas shift (WGS) reaction, $CO + H_2O \rightarrow CO_2 + H_2$, has attracted considerable interest, because of its potential application in the production of hydrogen for fuel cells.[1] WGS reaction is moderately exothermic with $\Delta H = -41.1\,kJ/mol$, thus low reaction temperature is beneficial for high CO conversion, while the kinetics is more favorable at high reaction temperatures. Currently, most attention has been focused on low-temperature WGS catalysts. An upstream high-temperature WGS catalyst with sufficient activity to achieve equilibrium with high flow rates is desirable, particularly for on-site or on-board hydrogen production for fuel cells. Conventional high-temperature WGS catalysts based on oxides of iron and chromium have been well established industrially, but further improvement is required for fuel-cell-oriented hydrogen production.[2] However, reports on high-temperature WGS catalysts under reforming condition are much fewer.[3] One crucial issue for high-temperature WGS reaction is methanation, $CO + 3H_2 \rightarrow CH_4 + H_2O$, $\Delta H = -205\,kJ/mol$ and $CO_2 + 4H_2 \rightarrow CH_4 + 2H_2O$, $\Delta H = -165\,kJ/mol$, which lead to hydrogen yield decrease and the temperature of catalyst bed increase, thereby lowering the efficiency of hydrogen production.[3,4]

In this work, nitric acid leached $Ni–CeO_2$ catalyst was applied for high-temperature WGS reaction, and the so prepared catalyst was highly active and selective for WGS reaction in reformate.

The coprecipitated $Ni–CeO_2$ catalysts were prepared by slowly adding a mixed aqueous solution of nickel nitrate and cerium nitrate and aqueous solution of NaOH and Na_2CO_3 with 1:1 molar ratio to deionized water under stirring and at a constant pH of 10 ± 0.1. The resultant precipitate was washed, dried at 80 °C and calcined in air at 400 °C for 4 h. The Ni metal content was 12.2 wt % which was measured by inductively coupled plasma atom emission spectroscopy (ICP-AES). The catalyst was denoted as $Ni–CeO_2$ (CP, 12.2 wt %). Single CeO_2 was prepared by the same method. Leaching by dilute nitric acid solutions, in order to remove weakly bound NiO from the $Ni–CeO_2$ (CP, 12.2 wt %) sample, was done by immersing the samples in 10% HNO_3 at room temperature for 24 h, then the resultant solid was washed with deionized water, dried at 80 °C and calcined in air at 400 °C for 1 h. The Ni metal content of leached sampales was 6.43 wt % which was also measured with ICP-AES. The leached sample was denoted as $Ni–CeO_2$ (L, 6.43 wt %). A commercial Fe–Cr catalyst (B110-2, Nanhua Chemic Inc) was used to benchmark the performance of the $Ni–CeO_2$ catalysts.

WGS reaction was performed at atmospheric pressure with a fixed bed flow reactor. Prior to each reaction tests, 100 mg of catalysts was reduced with a flow of 20% H_2/N_2 mixture at 400 °C for 1 h. Then, a simulated reforming mixture consisted of 4.97% CO, 7.50% CO_2, 20.84% H_2, 19.54% H_2O balanced with N_2 was introduced into the reactor at 400 °C and at a flow rate of 96 mL/min. Product gas streams were analyzed on-line with a gas chromatograph. Methane production was expressed as moles of CH_{4out}/(moles of CO_{in} + moles of CO_{2in}). CO conversion was expressed as (moles of CO_{in} − moles of CO_{out})/moles of CO_{in}.

The surface composition of the catalysts was determined by X-ray photoelectron spectroscopy (XPS, PE PHI-1600). The X-ray diffraction (XRD) patterns of the catalysts were recorded on a PANalytical X'Pert PRO XRD with Co radiation. Temperature-programmed reduction (TPR) of the catalysts was conducted in a fixed-bed continuous flow reactor–TCD system with reduction mixture of 5% H_2/Ar at a flow rate of 30 mL/min and at a heating rate of 10 °C/min.

Figure 1 showed catalytic performance over $Ni–CeO_2$ (CP, 12.2 wt %), $Ni–CeO_2$ (L, 6.43 wt %), and commercial Fe–Cr catalysts. Figure 1 also exhibited two WGS equilibrium curves for the simulated reforming conditions. The upper dashed line was the WGS equilibrium curve including the methanation reactions. The dotted line was the WGS equilibrium curve without methanation reactions. Both of the two $Ni–CeO_2$ catalysts were very active for CO conversion, while the product selectivity was very different. High methane production was observed over $Ni–CeO_2$ (CP, 12.2 wt %). On the other hand, $Ni–CeO_2$ (L, 6.43 wt %) was highly selective for WGS reaction and methanation was depressed markedly. In comparison with commercial Fe–Cr catalyst, $Ni–CeO_2$ (L, 6.43 wt %) was much more

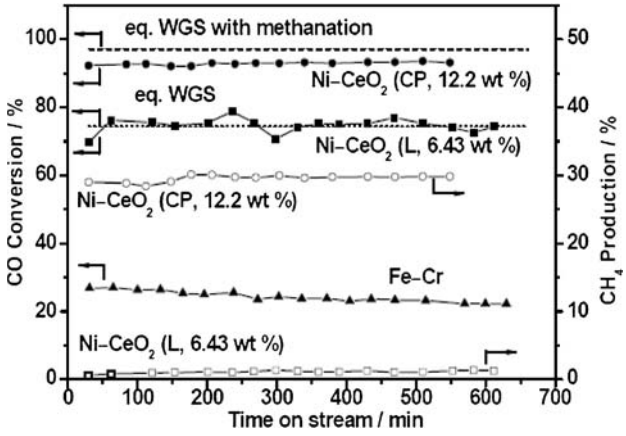

Figure 1. CO conversion and CH_4 production vs. reaction time over $Ni–CeO_2$ and commercial Fe–Cr catalysts for WGS reaction in simulated reforming mixture.

Table 1. Physical properties of CeO_2 and Ni–CeO_2

No.	Lattice parameter /nm	Crystallite sizes of CeO_2 /nm	Surface composition Ni/(Ni + Ce)/mol %
CeO_2	0.5405	8.3	—
Ni–CeO_2 (CP, 12.2 wt %)	0.5398	3.8	19.2
Ni–CeO_2 (L, 6.43 wt %)	0.5398	4.3	5.0

active. No obvious CH_4 was observed over the Fe–Cr catalyst.

Only fluorite oxide diffraction peaks of CeO_2 could be observed in XRD patterns for Ni–CeO_2 (CP, 12.2 wt %) and Ni–CeO_2 (L, 6.43 wt %) samples, and NiO phase could not be detected, suggesting that nickel oxide was in a highly dispersed or amorphous state. Table 1 listed some physical characters of CeO_2, Ni–CeO_2 (CP, 12.2 wt %), and Ni–CeO_2 (L, 6.43 wt %). As could be seen from this table, the lattice parameters of CeO_2 decreased with the addition of Ni, suggesting the incorporation of nickel ions into the CeO_2 lattice and the formation of the solid solution of $Ce_{1-X}Ni_XO_2$, since the size of nickel ions was smaller than that of Ce^{4+} ions.[5] The lattice parameter of CeO_2 in Ni–CeO_2 (CP, 12.2 wt %) was the same with that in Ni–CeO_2 (L, 6.43 wt %), indicating that the incorporated nickel ions were not removed in the nitric-acid-leaching process. The mean crystallite size of CeO_2 decreased obviously with adding of nickel species, suggesting that thermal stability of CeO_2 was improved by adding nickel. A small increase in crystallite size, from 3.8 to 4.3 nm, due to nitric acid leaching was observed, which should be caused by the sintering in the calcination following the leaching. The surface composition Ni/(Ni + Ce) of the Ni–CeO_2 (L, 6.43 wt %) was lower than that of the Ni–CeO_2 (CP, 12.2 wt %), which should be ascribed to the removal of nickel oxide by leaching.

Figure 2 showed the TPR profiles of Ni–CeO_2 (CP, 12.2 wt %) and Ni–CeO_2 (L, 6.43 wt %) samples. Ni–CeO_2 (CP, 12.2 wt %) gave three hydrogen consumption peaks (α_1, α_2, and β). The α_1 and α_2 peaks located at temperatures lower than 300 °C was ascribed to the reduction of adsorbed oxygen species at CeO_2 vacancies, while the high-temperature peak, at 380 °C (β), resulted from the reduction of NiO.[5] It is generally accepted that the solid solution of $Ce_{1-X}Ni_XO_2$ can be formed by the incorporation of Ni^{2+} ions into CeO_2 lattice in Ni–CeO_2 system. The incorporation leads to unbalance of electrical charge and lattice distortion of CeO_2, resulting in the generation of oxygen vacancies and adsorbing of oxygen species on the vacancies which is reducible by H_2 at low temperature. Compared with Ni–CeO_2 (CP, 12.2 wt %) catalyst, the relative intensity of α_1 and α_2 peaks changed little in TPR profiles of Ni–CeO_2 (L, 6.43 wt %), but the β peak disappeared. The results indicated that the weakly bound nickel oxide had been removed effectively from the sample by dilute nitric acid leaching, but the Ni^{2+} ions incorporated into CeO_2 lattice did not removed by the leaching. This is consistent with the results of ICP-AES, XRD, and XPS.

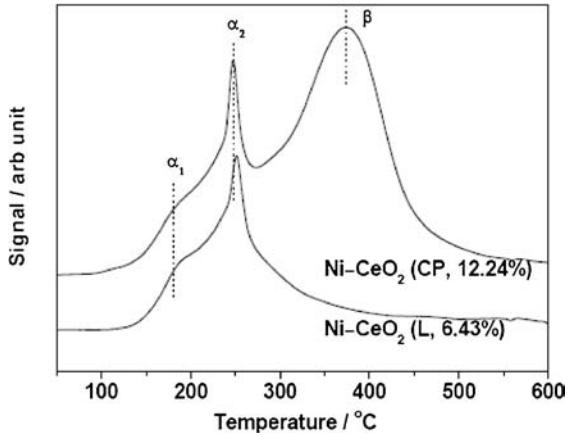

Figure 2. TPR patterns of Ni–CeO_2 catalysts.

Recently, Au/CeO_2, Pt/CeO_2, and Cu/CeO_2 catalysts have been reported to be very promising for WGS reaction owing to the redox properties of CeO_2 and its oxygen storage capacity.[6] As for active sites on metal–ceria catalysts for WGS reaction, either reduced metal nanoparticles or atomically dispersed cationic metal species have been proposed as active sites for the WGS reaction, and it is widely accepted that oxygen vacancies are essential for the activation of water.[6] In the present study, by correlating catalytic performance with TPR and XRD results, it was proposed that the highly dispersed metal Ni particles were the active sites for methane production and that the Ni^{2+} ions, incorporated into CeO_2 lattice and surrounded by oxygen vacancies, were the key active sites for WGS reaction. The superior catalytic activity and selectivity of the Ni–CeO_2 (L, 6.43 wt %) catalyst for WGS reaction were attributed to the presence of high amounts of Ni^{2+} ions incorporated into CeO_2 lattice and the absence of Ni metal particles on the catalytic surface.

The authors would like to acknowledge National Natural Science Foundation of China (Granted as No. 20476079) and the Cheung Kong Scholar Program for Innovative Teams of the Ministry of Education (No. IRT0641) for financial support of this work.

References

1 a) D. L. Trimm, Z. I. Önsan, *Catal. Rev.* **2001**, *43*, 31. b) A. F. Ghenciu, *Curr. Opin. Solid State Mater. Sci.* **2002**, *6*, 389.
2 C. Rhodes, B. P. Williams, F. King, G. J. Hutchings, *Catal. Commun.* **2002**, *3*, 381.
3 a) P. Kumar, R. Idem, *Energy Fuels* **2007**, *21*, 522. b) C. M. Y. Yeung, F. Meunier, R. Burch, D. Thompsett, S. C. Tsang, *J. Phys. Chem. B* **2006**, *110*, 8540.
4 C. Wheeler, A. Jhalani, E. J. Klein, S. Tummala, L. D. Schmidt, *J. Catal.* **2004**, *223*, 191.
5 a) W. Shan, M. Luo, P. Ying, W. Shen, C. Li, *Appl. Catal. A* **2003**, *246*, 1. b) N. Yi, Y. Cao, Y.-M. Liu, W.-L. Dai, H.-Y. He, K.-N. Fan, *Chem. Lett.* **2005**, *34*, 108.
6 a) Q. Fu, H. Saltsburg, M. Flytzani-Stephanopoulos, *Science* **2003**, *301*, 935. b) X. Wang, J. A. Rodriguez, J. C. Hanson, D. Gamarra, A. Martínez-Arias, M. Fernández-García, *J. Phys. Chem. B* **2006**, *110*, 428. c) G. Jacobs, S. Ricote, B. H. Davis, *Appl. Catal. A* **2006**, *302*, 14. d) C. H. Kim, L. T. Thompson, *J. Catal.* **2006**, *244*, 248.

Published on the web (Advance View) December 15, 2007; doi:10.1246/cl.2008.74